

Bragg scattering of an ultracold dipolar gas across the phase transition from Bose-Einstein condensate to supersolid in the free-particle regime

D. Petter ¹, A. Patscheider ¹, G. Natale,¹ M. J. Mark ^{1,2}, M. A. Baranov,^{2,3} R. van Bijnen,^{2,3} S. M. Rocuzzo,^{4,5} A. Recati,^{4,5} B. Blakie,^{6,7} D. Baillie ^{6,7}, L. Chomaz,¹ and F. Ferlaino^{1,2,*}

¹*Institut für Experimentalphysik, Universität Innsbruck, Technikerstraße 25, 6020 Innsbruck, Austria*

²*Institut für Quantenoptik und Quanteninformation, Österreichische Akademie der Wissenschaften, Technikerstraße 21a, 6020 Innsbruck, Austria*

³*Center for Quantum Physics, University of Innsbruck, 6020 Innsbruck, Austria*

⁴*INO-CNR BEC Center and Dipartimento di Fisica, Università degli Studi di Trento, 38123 Povo, Italy*

⁵*Trento Institute for Fundamental Physics and Applications, INFN, 38123 Trento, Italy*

⁶*The Dodd-Walls Centre for Photonic and Quantum Technologies, University of Otago, Dunedin 9054, New Zealand*

⁷*Department of Physics, University of Otago, Dunedin 9016, New Zealand*



(Received 5 May 2020; revised 30 March 2021; accepted 9 June 2021; published 22 July 2021)

We present an experimental and theoretical study of the response of a dipolar supersolid to a Bragg excitation at high-energy defined by the impulse approximation regime. We experimentally observe a continuous reduction of the response when tuning the contact interaction from an ordinary Bose-Einstein condensate to a supersolid state and ultimately to an incoherent array of droplets. Already in the supersolid regime, the observed reduction is faster than the one theoretically predicted by the Bogoliubov–de Gennes theory. By comparing experiments and theories, we are able to attribute this discrepancy to the presence of coherent phase dynamics induced by the crossing of the phase transition. The phase variations are found to change character along the phase diagram and become predominantly incoherent only when reaching the incoherent-droplet regime.

DOI: [10.1103/PhysRevA.104.L011302](https://doi.org/10.1103/PhysRevA.104.L011302)

Recently, supersolid states have been realized in laboratories using ultracold quantum gases of dipolar atoms [1–3]. Predicted more than half a century ago [4–7] and long searched for in helium [8], this intriguing phase of matter spontaneously breaks two symmetries, namely the translational and the gauge symmetry. The breaking of the former one gives rise to a periodic order in space with the system ground state developing a density modulation, recalling a crystalline structure, whereas the breaking of the gauge symmetry introduces a superfluid flow of particles.

The supersolid phase (SSP) transition is typically controlled by the interaction. By varying its strength, a quantum system may pass from an unmodulated superfluid to a fully localized crystal state of insulating droplets (ID). Between these two extremes, the system is supersolid, showing a coexistence of these two apparently antithetical orders. The interplay between localization and superfluidity has raised lively debates [4–7]. In a seminal work, Leggett derived an upper-bound relation for the superfluid fraction in a supersolid [9], which directly connects the loss of superfluidity with the increase of localization, the latter being quantified in terms of a modulation contrast. Importantly, Leggett’s famous formula is valid at equilibrium and requires the macroscopic phase of the quantum system to be stationary.

However, in experiments, a common path to create dipolar supersolids relies on interaction tuning [1–3,10–13]. The corresponding dynamical crossing of the phase transition may introduce excitations, which, on the one hand, naturally questions the applicability of equilibrium theories. On the other hand, excitations typically entail phase variations, raising interest in understanding their role and impact on the system behavior, calling for the development of theoretical models accounting for out-of-equilibrium effects.

Interestingly, phase variations across the system display different natures. They can be coherent and deterministic, or incoherent and random depending whether they arise from collective dynamics or, e.g., from quantum and thermal fluctuations. While experiments pointed to the existence of phase variations in dipolar supersolids [11–13], a comprehensive study of their characteristics and origins is lacking. Providing access to local properties of the system, high-energy scattering measurements may help by bridging this gap. Such scattering protocols have been successfully used across a vast range of disciplines, from high-energy [14–17] to condensed-matter physics [18,19]. They allowed measurements, e.g., of the condensate fraction in superfluid liquid helium [20] and of beyond-mean-field effects in ultracold gases [21–27].

In this Letter, we study the response of a dipolar supersolid to a high-energy two-photon Bragg scattering probe. As the system crosses from the Bose-Einstein condensate (BEC) into the SSP, we observe a strong reduction of the scattering response, that eventually vanishes in the ID regime. A comparison with theory reveals that the response is reduced

* Author to whom correspondence and requests for materials should be addressed: Francesca.ferlaino@uibk.ac.at

stronger than expected from the emergence of a density modulation in the SSP. Going beyond equilibrium expectations, we find that coherent phase variations, emerging due to the crossing of the BEC-SSP transition, are the cause of the anomalous response suppression.

We start by reviewing the description of the dynamical response of an interacting many-body system to a weak scattering probe within the linear-response theory [28]. The dynamic structure factor (DSF), $S(\mathbf{k}, \omega)$, quantifies the density response of a system to a probe of momentum, $\hbar\mathbf{k}$, and energy, $\hbar\omega$. For weak interactions at equilibrium, the DSF is related to the excitation spectrum via the Bogoliubov amplitudes, u_j and v_j , describing the excitation mode j of energy $\hbar\omega_j$. It reads

$$S(\mathbf{k}, \omega) = \sum_j \left| \int d\mathbf{r} (u_j^*(\mathbf{r}) + v_j^*(\mathbf{r})) e^{i\mathbf{k}\cdot\mathbf{r}} \psi_0(\mathbf{r}) \right|^2 \times \delta(\hbar\omega - \hbar\omega_j), \quad (1)$$

where we neglect the creation of multiple excitations. Here, ψ_0 is the system's macroscopic ground-state wave function.

Equation (1) gives different information depending on the momentum and energy ranges [28]: For low- \mathbf{k} transfer, $S(\mathbf{k}, \omega)$ is sensitive to the system's collective response, whereas, in the high- \mathbf{k} and high-energy regime, the DSF is proportional to the momentum distribution of the system, $\tilde{n}(\mathbf{k})$. Here, we focus on the latter regime to probe the impact of density modulation in a superfluid state. We study the response along the density-modulated direction, y , with $\mathbf{k} = (0, k_y, 0)$. In the regime of free-particle excitations ($u_j \rightarrow e^{ik_j y}$, $v_j \rightarrow 0$, $\omega_j \rightarrow \hbar k_j^2/2m$ with m the atomic mass), the impulse approximation becomes valid and we find [28–32]

$$S(k_y, \omega) = \sum_j \tilde{n}(0, k_y - k_j, 0) \delta(\hbar\omega - \hbar\omega_j). \quad (2)$$

On resonance, $\omega = \omega_j$ and $k_y = k_j$, the DSF is uniquely determined by the system's momentum distribution at $\mathbf{k} = 0$, independent on the probed momentum k_j , $S(k_j) \equiv S(k_j, \omega_j) \propto \tilde{n}(\mathbf{k} = 0)$.

To identify the free-particle regime, we calculate the excitation spectrum. Following the Bogoliubov–de Gennes (BdG) theory, a free-particle excitation is an elementary excitation of plane wave character. This occurs for excitations of high enough energy and single-particle character ($\|u_j\| = \int |u_j(\mathbf{r})|^2 d\mathbf{r} = 1$ and $\|v_j\| = 0$) [28,33].

In order to gain an intuition, we begin with calculating the Bogoliubov amplitudes and $S(\mathbf{k}, \omega)$ in the thermodynamic limit. We consider the BdG theory for an infinitely elongated erbium quantum gas. As shown in Figs. 1(a) and 1(b), the supersolid spectrum exhibits a periodic structure in momentum space with a period given by the reciprocal lattice vector k_c . The state develops a density modulation along the axial direction with wavelength $2\pi/k_c$ [see inset in Fig. 1(b)]. The two lowest branches correspond to the superfluid and crystal branches, respectively [35]. At higher energies, excitations follow a gapped parabolic dispersion branch and a flat band at $\omega \approx 1.25\omega_z$ (corresponding to transverse breathing modes of single-droplets). Importantly, the excitation modes of the parabolic branch have a free-particle character, when $\|u\| = 1$.

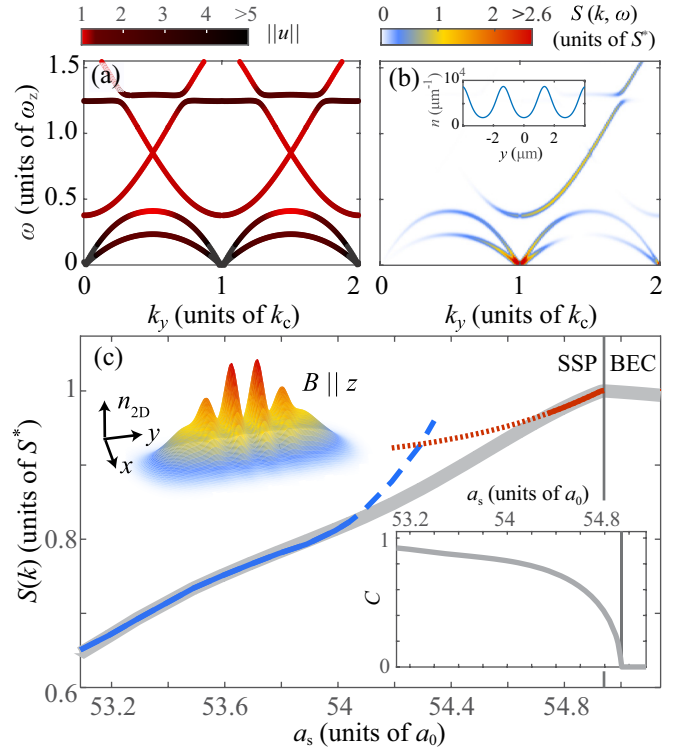


FIG. 1. (a) Axial excitation spectrum of the transversely symmetric modes and (b) corresponding DSF of an infinitely elongated dipolar supersolid at $a_s = 51 a_0$ in a harmonic trap with $\omega_{x,y,z} = 2\pi \times (250, 0, 160)$ Hz. The color maps correspond to $\|u\|$ and $S(k, \omega)$, respectively. The inset shows the integrated axial density profile $n(y)$ of the ground state with mean density $4.7 \times 10^3 \mu\text{m}^{-1}$. (c) $S(k)$ for the 3D-trapped system with $\omega_{x,y,z} = 2\pi \times (250, 31, 160)$ Hz. $S(k)$ is calculated at $k = 4.2 \mu\text{m}^{-1} \approx 1.8 k_c$ (grey line) and normalized by its value at the BEC-SSP phase transition, S^* . The atom number is varied with a_s to match the experimental conditions [34]. The red (blue) line shows the result from the SIA (DAA). (upper inset) Integrated density profile of the ground state at $a_s = 54.49 a_0$ and $N = 5 \times 10^4$ atoms. (lower inset) Evolution of the ground state's central contrast C . For the infinite (3D-trapped) case, $k_c = 2.3 \mu\text{m}^{-1} (2.4 \mu\text{m}^{-1})$.

We now move on to the three-dimensional (3D) trapped case for the experimentally relevant parameters. Previous works have shown that the main spectral features qualitatively persist when changing from the infinite to the finite sized system [10–12,36,37]. We calculate the spectrum of excitations as in Refs. [10,38] and extract the Bogoliubov amplitudes. Similar to the infinite system, we find a free-particle character for excitations with $\hbar\omega \gtrsim 0.6 \hbar\omega_z$ [34]. This enables the impulse approximation for the later experiments, which are done at an exemplary momentum of $k \approx 1.8 k_c$. Figure 1(c) shows $S(k \approx 1.8 k_c)$, which decreases when entering the SSP from the BEC and further reduces when lowering a_s . Simultaneously, the ground-state density develops a spatial modulation (upper inset), whose contrast C rapidly increases (lower inset). Note that C evolves faster with a_s than $S(k)$. For instance, at $a_s = 53 a_0$, $C \approx 1$, whereas $S(k)$ reduces only by about 35%. Here, $C = (n_{\text{max}} - n_{\text{min}})/(n_{\text{max}} + n_{\text{min}})$ with n_{max} (n_{min})

being the central maximum (minimum) of the integrated density [34].

To gain an intuitive understanding of the density-response reduction, we develop a 1D model [32]. Using two different wave-function ansatzes, we evaluate $S(k)$ in the weak and strong density-modulation regimes. As discussed in Refs. [39–41], for weakly modulated supersolids, with $C \ll 1$, the ground-state wave function can be approximated by a fully coherent sine-modulated function on top of a uniform background. At leading order in C , it reads $\psi(y) = \sqrt{n}(1 + C \sin(k_c y)/2)$, with n being the mean density. Applying this sine ansatz (SIA) in Eq. (2), we find $S(k) \propto n(1 - C^2/8)$. This result shows that an increasing contrast directly causes a suppression of the DSF. We find a similar C dependence for the superfluid fraction derived from Leggett’s formula [9], $f_{\text{SF}} = 1 - C^2/2$. Therefore, in the weakly modulated regime, the reduction of the high-energy scattering response connects to the reduction of the superfluid fraction [32]. We benchmark our SIA results with the BdG calculations for an equilibrium supersolid state, by evaluating C from the full Gross-Pitaevskii equation (GPE) solution [34]. As shown in Fig. 1(c), despite its simplicity, the SIA scaling reproduces very well the full numerics up to $C \lesssim 40\%$. For larger C , as expected, the model breaks down.

For large C , we employ a droplet-array ansatz (DAA), describing the system as an array of N_D droplets, $\psi(y) = \sum_{j=1}^{N_D} \chi(y - jd)e^{i\theta_j}$ [3,42]. Each droplet is described by a Gaussian function, $\chi(y)$, of size σ , separated by a distance $d > \sigma$ from its neighbours. Each droplet is allowed to have an independent, yet uniform, phase θ_j . Within the DAA, the DSF shows the proportionality $S(k) \propto n |\frac{1}{N_D} \sum_{j=1}^{N_D} e^{i\theta_j}|^2 \sigma/d$. It decreases with both the density overlap between droplets, set by σ/d , and the phase variance along the array. The phase variance can not be accounted for in the ground-state GPE theory, which describes a state possessing a uniform phase. To benchmark the DAA results with the BdG calculations, we thus set $\theta_j = 0$ for all j [34]. We find a very good agreement for $C > 80\%$. The effect of phase variations on the scattering response will be later studied using dynamical simulations; see Figs. 3 and 4.

To summarize, at equilibrium, the high-energy response decreases when the contrast increases. For a small density modulation, the response can be directly connected to Leggett’s estimate for the superfluid fraction. Moreover, the presence of phase variations further decreases the response, as we explicitly show using the DAA. We now compare our theory expectation with the experiment.

In the experiments, we access the density response of a supersolid by performing high-energy Bragg scattering on a ^{166}Er dipolar quantum gas, confined in an axially elongated harmonic trap. A transverse homogeneous magnetic field orients the atomic dipoles and sets a_s [3]. We initially prepare the system in the ordinary BEC phase, and enter the SSP via interaction tuning by linearly lowering a_s below a critical value, a_s^* , for which the BEC-SSP phase transition occurs. Similar to previous experiments [3,10], a_s^* is extracted with an interferometric technique. For the present trap and atom numbers, N , we measure $a_s^* = 54.94_{-13}^{+28} a_0$. Furthermore, we observe the ID regime below $a_s \approx 53.9 a_0$, see Ref. [34].

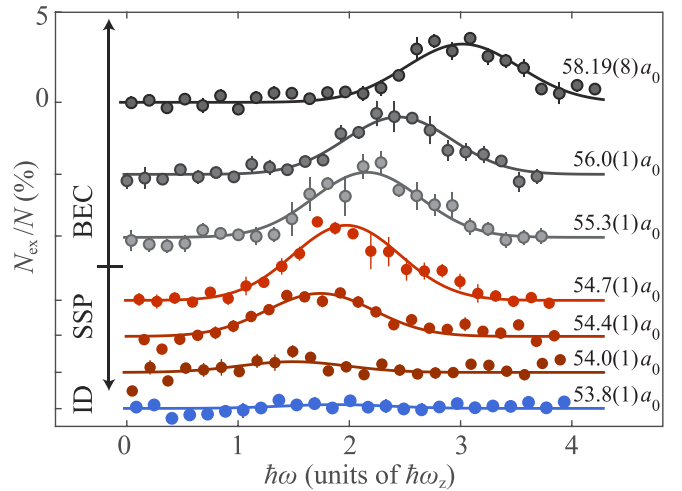


FIG. 2. Fraction of Bragg-excited atoms as a function of ω for various a_s across the BEC-SSP-ID regimes (see labels). The spectra are vertically offset for visibility. Here and throughout the Letter, the error bars correspond to one standard error. Solid lines show the Gaussian fits to the data.

For the Bragg excitation, we project on the atoms an optical lattice potential of constant depth V for a duration $\tau = 7$ ms. The lattice has a constant wave vector $k = 4.2(3)\mu\text{m}^{-1}$ along y and moves with a variable frequency ω . After the Bragg excitation, we measure the integrated momentum distribution, $\tilde{n}(k_x, k_y)$, using a time-of-flight expansion of 30 ms. The number of excited atoms N_{exc} is extracted in a narrow region of interest around k [34]. For a fixed a_s , we find a clear resonance in N_{exc}/N as we vary ω . From a Gaussian fit we extract the resonance peak’s amplitude, \mathcal{F} . From linear response theory, we expect $\mathcal{F} \propto V^2 \tau S(k)$ [43]. For the relevant a_s range, we

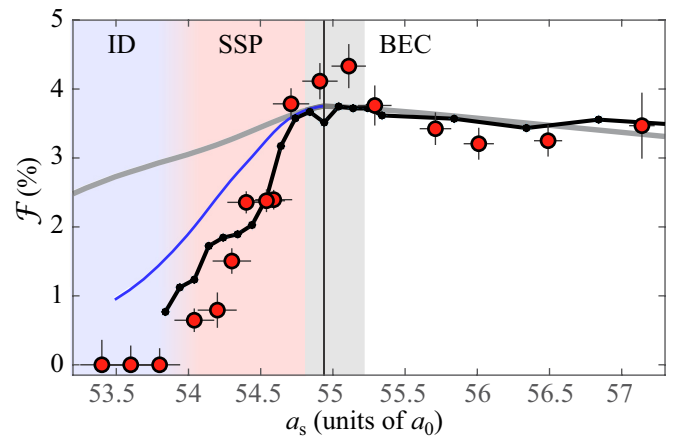


FIG. 3. Experimental \mathcal{F} (circles) versus a_s across the BEC-SSP-ID phases. For the lowest three a_s , we do not observe a resonance and plot the standard deviation of the data as an error estimate. Horizontal error bars correspond to uncertainties of the magnetic field [34]. Theoretical \mathcal{F} (lines) from the BdG calculations on the ground state (grey), from the RTE simulations (black), and from the rescaled BdG calculations that include $\Delta\Theta$ obtained from the RTE (blue). The gray shading corresponds to the uncertainty in a_s of the experimental phase transition (vertical line).

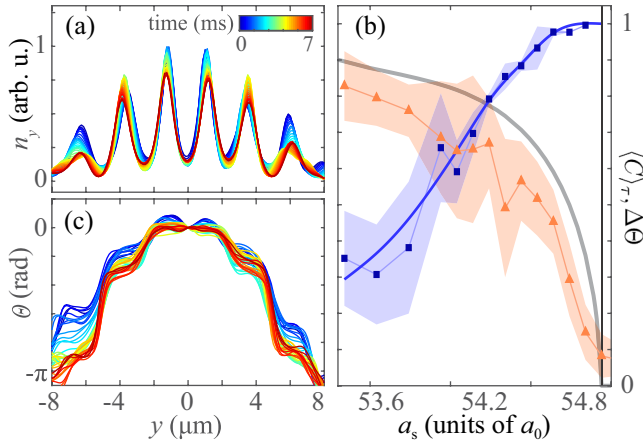


FIG. 4. RTE simulations without Bragg excitation. (a) Time evolution of the integrated *in situ* density of the wave function for $a_s = 54.04 a_0$. (b) $\langle C \rangle_\tau$ (triangles) and $\Delta\Theta$ (squares) versus a_s . The grey line corresponds to the central contrast obtained from the ground-state theory. The solid blue line is a smooth interpolation of $\Delta\Theta$, fixed to unity at the phase transition point. The shadings give the standard deviation obtained from five simulation runs. The vertical line corresponds to the phase transition point. (c) Phase cuts corresponding to the simulation shown in (a).

have checked the scaling with τ and V [34]. Figure 2 shows examples of the Bragg-excitation spectrum for various a_s . In the BEC regime until the onset of the SSP, we observe a downward shift of the resonance frequency without a significant change in \mathcal{F} [34]. In contrast, as we enter into the SSP regime, \mathcal{F} undergoes a stark reduction. In the ID regime, the resonance peak completely vanishes.

Figure 3 shows the evolution of \mathcal{F} across the BEC-SSP-ID phase diagram. The a_s extension of the three phases (see background colors), has been determined from independent measurements of the phase coherence and density modulation of the states [3,34]. When reducing a_s , \mathcal{F} first slightly increases in the BEC phase, continuously crosses at the BEC-SSP transition, and then drastically reduces to $\lesssim 1\%$, close to our detection level, when lowering a_s further by $\sim 0.5 a_0$. Finally, for $a_s < 54 a_0$, we do not observe any resonant response.

We compare the experimental results with our BdG theory for the stationary, trapped gas. While in the BEC regime, experiment and theory show a good agreement, in the SSP they start to substantially deviate from each other. The data shows a much faster reduction of \mathcal{F} than the one predicted by the BdG theory. This suggests that an important ingredient is missing in the ground-state theory. Our DAA model provides a first intuitive explanation, showing that, not only the increasing crystalline modulation but also phase variations can lead to a reduction of the system response. We envision two sources of phase variations. First, quantum and thermal fluctuations, which are expected to dominate in the ID regime, yield phase patterns varying from shot to shot. Second, coherent dynamics, as, e. g., induced by the crossing of the BEC-SSP phase transition, leading to reproducible phase patterns. Neither phenomena are accounted for in the BdG calculations.

To investigate these effects, we simulate the system real-time evolution (RTE) [44]. Our calculations reproduce the full

experimental sequence [34]. Random shot-to-shot variations are included by adding an initial population of BdG modes from quantum and thermal noises [34]. From the simulated momentum distributions, we extract the excited fractions, as done for the experimental data. Contrary to the BdG results, the RTE simulations describe remarkably well the data both in the BEC and SSP phase; see Fig. 3.

The impact of the changing contrast and phase variations across SSP-ID phase can be seen from RTE without a Bragg excitation for different holding times. As shown in Fig. 4(a), the density profiles $n(y)$ exhibit only a slight reduction of the contrast with time due to atom loss. As expected, the calculated $\langle C \rangle_\tau$, time averaged over the Bragg scattering duration, increase with decreasing a_s . However, for each a_s , we observe a 10–30 % lower contrast than the one extracted from the ground-state calculations. Since a reduced contrast would mean an increase in \mathcal{F} , the varying contrast cannot explain the mismatch between the BdG theory and both the experimental and RTE results; see Fig. 3.

The RTE calculations also reveal that the phase of the wave function, $\theta(y)$, develops a nonuniform profile. For instance at $a_s = 54.04 a_0$, $\theta(y)$ exhibits a stairlike profile with fairly constant values within the density peaks and discrete phase steps in between them; see Fig. 4(c). This behavior suggests that each density peak acquires an independent phase, despite their density links. We also observe that the phase pattern is fairly reproducible between simulation runs and mainly affected by the coherent dynamics arising by the crossing of the phase transition [34].

Following the DAA model, phase variations are expected to reduce $S(k)$ by a factor $\Delta\Theta \approx |\frac{1}{N_b} \sum_{j=1}^{N_b} \langle e^{i\theta_j} \rangle_\tau|^2$ [28,34]. As shown in Fig. 4(b), $\Delta\Theta$ is almost unity close to the BEC-SSP phase transition and significantly drops when lowering a_s towards the ID regime, where it starts to flatten. The standard deviation of $\Delta\Theta$ relates to the shot-to-shot reproducibility of the phase pattern. In the SSP, the deviation remains small, confirming that the phase variations originate from coherent dynamics. In contrast, the deviation increases when reaching the ID regime. This highlights the increasing effects of fluctuations, showing that the phase variations ultimately become incoherent. We empirically account for the effect of phase variations in the BdG theory by scaling the DSF with $\Delta\Theta$ over the whole SSP-ID regimes. As shown in Fig. 3, this simple inclusion of $\Delta\Theta$ shows the pronounced impact of the coherent phase variations for the experimentally observed response.

In conclusion, we demonstrate high-energy two-photon Bragg scattering spectroscopy as a sensitive probe of density modulations, and coherent and incoherent phase variations in a quantum system. Accounting for the phase variations is crucial to fully capture the behavior of supersolid states created in experiments via a dynamical tuning of the interactions. Our work provides important steps to a more complete vision of the dipolar supersolid, including out-of-equilibrium phenomena, and opens the door for future exploration of critical phenomena induced by the dynamical crossing of the BEC-SSP phase transition [45–47].

We thank S. Stringari for insightful discussions and B. Yang for the careful reading of the manuscript. Part of the computational results presented have been achieved using

the HPC infrastructure LEO of the University of Innsbruck. This work is financially supported through an ERC Consolidator Grant (RARE, No. 681432), a DFG/FWF (FOR 2247/PI2790) and a joint-project grant from the FWF (No. I 4426, RSF/Russland 2019). L. C. acknowledges the

support of the FWF via the Elise Richter Fellowship number V792. A. R. and S. M. R. acknowledge support from Provincia Autonoma di Trento and the Q@TN initiative. We also acknowledge the Innsbruck Laser Core Facility, financed by the Austrian Federal Ministry of Science, Research and Economy.

- [1] L. Tanzi, E. Lucioni, F. Famà, J. Catani, A. Fioretti, C. Gabbanini, R. N. Bisset, L. Santos, and G. Modugno, *Phys. Rev. Lett.* **122**, 130405 (2019).
- [2] F. Böttcher, J.-N. Schmidt, M. Wenzel, J. Hertkorn, M. Guo, T. Langen, and T. Pfau, *Phys. Rev. X* **9**, 011051 (2019).
- [3] L. Chomaz, D. Petter, P. Ilzhöfer, G. Natale, A. Trautmann, C. Politi, G. Durastante, R. M. W. van Bijnen, A. Patscheider, M. Sohmen, M. J. Mark, and F. Ferlaino, *Phys. Rev. X* **9**, 021012 (2019).
- [4] O. Penrose and L. Onsager, *Phys. Rev.* **104**, 576 (1956).
- [5] E. P. Gross, *Phys. Rev.* **106**, 161 (1957).
- [6] A. F. Andreev and I. M. Lifshitz, *Zh. Eksp. Teor. Fiz.* **56**, 2057 (1969) [*Sov. Phys. JETP* **29**, 1107 (1969)].
- [7] G. V. Chester, *Phys. Rev. A* **2**, 256 (1970).
- [8] S. Balibar, *Nature (London)* **464**, 176 (2010).
- [9] A. J. Leggett, *Phys. Rev. Lett.* **25**, 1543 (1970).
- [10] G. Natale, R. M. W. van Bijnen, A. Patscheider, D. Petter, M. J. Mark, L. Chomaz, and F. Ferlaino, *Phys. Rev. Lett.* **123**, 050402 (2019).
- [11] L. Tanzi, S. M. Roccuzzo, E. Lucioni, F. Famà, A. Fioretti, C. Gabbanini, G. Modugno, A. Recati, and S. Stringari, *Nature (London)* **574**, 382 (2019).
- [12] M. Guo, F. Böttcher, J. Hertkorn, J.-N. Schmidt, M. Wenzel, H. P. Büchler, T. Langen, and T. Pfau, *Nature (London)* **574**, 386 (2019).
- [13] L. Tanzi, J. G. Maloberti, G. Biagioni, A. Fioretti, C. Gabbanini, and G. Modugno, *Science* **371**, 1162 (2021).
- [14] R. E. Taylor, *Rev. Mod. Phys.* **63**, 573 (1991).
- [15] H. W. Kendall, *Rev. Mod. Phys.* **63**, 597 (1991).
- [16] J. I. Friedman, *Rev. Mod. Phys.* **63**, 615 (1991).
- [17] M. Breidenbach, J. I. Friedman, H. W. Kendall, E. D. Bloom, D. H. Coward, H. DeStaebler, J. Drees, L. W. Mo, and R. E. Taylor, *Phys. Rev. Lett.* **23**, 935 (1969).
- [18] A. Griffin, *Excitations in a Bose-Condensed Liquid* (Cambridge University Press, New York, 1993).
- [19] C. Giacovazzo, H. L. Monaco, D. Viterbo, F. Scordari, G. Gilli, G. Zanotti, and M. Catti, *Fundamentals of Crystallography* (Oxford University Press, Oxford, 1992).
- [20] T. R. Sosnick, W. M. Snow, P. E. Sokol, and R. N. Silver, *Europhys. Lett.* **9**, 707 (1989).
- [21] S. Richard, F. Gerbier, J. H. Thywissen, M. Hugbart, P. Bouyer, and A. Aspect, *Phys. Rev. Lett.* **91**, 010405 (2003).
- [22] T. Stöferle, H. Moritz, C. Schori, M. Köhl, and T. Esslinger, *Phys. Rev. Lett.* **92**, 130403 (2004).
- [23] S. B. Papp, J. M. Pino, R. J. Wild, S. Ronen, C. E. Wieman, D. S. Jin, and E. A. Cornell, *Phys. Rev. Lett.* **101**, 135301 (2008).
- [24] E. D. Kuhnle, H. Hu, X.-J. Liu, P. Dyke, M. Mark, P. D. Drummond, P. Hannaford, and C. J. Vale, *Phys. Rev. Lett.* **105**, 070402 (2010).
- [25] N. Fabbri, D. Clément, L. Fallani, C. Fort, and M. Inguscio, *Phys. Rev. A* **83**, 031604(R) (2011).
- [26] S. Hoinka, M. Lingham, K. Fenech, H. Hu, C. J. Vale, J. E. Drut, and S. Gandolfi, *Phys. Rev. Lett.* **110**, 055305 (2013).
- [27] R. Lopes, C. Eigen, A. Barker, K. G. H. Viebahn, M. Robert-de Saint-Vincent, N. Navon, Z. Hadzibabic, and R. P. Smith, *Phys. Rev. Lett.* **118**, 210401 (2017).
- [28] L. Pitaevskii and S. Stringari, *Bose-Einstein Condensation and Superfluidity* (Oxford University Press, Oxford, 2016), Vol. 164.
- [29] P. C. Hohenberg and P. M. Platzman, *Phys. Rev.* **152**, 198 (1966).
- [30] F. Zambelli, L. Pitaevskii, D. M. Stamper-Kurn, and S. Stringari, *Phys. Rev. A* **61**, 063608 (2000).
- [31] J. Hofmann and W. Zwerger, *Phys. Rev. X* **7**, 011022 (2017).
- [32] L. Chomaz, *Phys. Rev. A* **102**, 023333 (2020).
- [33] S. Ronen, D. C. E. Bortolotti, and J. L. Bohn, *Phys. Rev. A* **74**, 013623 (2006).
- [34] See Supplemental Material at <http://link.aps.org/supplemental/10.1103/PhysRevA.104.L011302>, which includes Refs. [48–55] and details on the analysis and theory calculations.
- [35] S. Saccani, S. Moroni, and M. Boninsegni, *Phys. Rev. Lett.* **108**, 175301 (2012).
- [36] J. Hertkorn, F. Böttcher, M. Guo, J. N. Schmidt, T. Langen, H. P. Büchler, and T. Pfau, *Phys. Rev. Lett.* **123**, 193002 (2019).
- [37] S. M. Roccuzzo and F. Ancilotto, *Phys. Rev. A* **99**, 041601(R) (2019).
- [38] D. Petter, G. Natale, R. M. W. van Bijnen, A. Patscheider, M. J. Mark, L. Chomaz, and F. Ferlaino, *Phys. Rev. Lett.* **122**, 183401 (2019).
- [39] P. B. Blakie, D. Baille, L. Chomaz, and F. Ferlaino, *Phys. Rev. Research* **2**, 043318 (2020).
- [40] Z.-K. Lu, Y. Li, D. S. Petrov, and G. V. Shlyapnikov, *Phys. Rev. Lett.* **115**, 075303 (2015).
- [41] N. Sepúlveda, C. Jossierand, and S. Rica, *Phys. Rev. B* **77**, 054513 (2008).
- [42] M. Wenzel, F. Böttcher, T. Langen, I. Ferrier-Barbut, and T. Pfau, *Phys. Rev. A* **96**, 053630 (2017).
- [43] P. B. Blakie, R. J. Ballagh, and C. W. Gardiner, *Phys. Rev. A* **65**, 033602 (2002).
- [44] L. Chomaz, R. M. W. van Bijnen, D. Petter, G. Faraoni, S. Baier, J. H. Becher, M. J. Mark, F. Wächtler, L. Santos, and F. Ferlaino, *Nat. Phys.* **14**, 442 (2018).
- [45] T. W. B. Kibble, *J. Phys. A* **9**, 1387 (1976).
- [46] W. H. Zurek, *Nature (London)* **317**, 505 (1985).
- [47] J. Eisert, M. Friesdorf, and C. Gogolin, *Nat. Phys.* **11**, 124 (2015).
- [48] L. Chomaz, S. Baier, D. Petter, M. J. Mark, F. Wächtler, L. Santos, and F. Ferlaino, *Phys. Rev. X* **6**, 041039 (2016).

- [49] P. L. Gould, G. A. Ruff, and D. E. Pritchard, *Phys. Rev. Lett.* **56**, 827 (1986).
- [50] I. Bloch, J. Dalibard, and W. Zwerger, *Rev. Mod. Phys.* **80**, 885 (2008).
- [51] L. Santos, G. V. Shlyapnikov, and M. Lewenstein, *Phys. Rev. Lett.* **90**, 250403 (2003).
- [52] D. H. J. O'Dell, S. Giovanazzi, and G. Kurizki, *Phys. Rev. Lett.* **90**, 110402 (2003).
- [53] T. Macrì, F. Maucher, F. Cinti, and T. Pohl, *Phys. Rev. A* **87**, 061602(R) (2013).
- [54] F. Böttcher, M. Wenzel, J.-N. Schmidt, M. Guo, T. Langen, I. Ferrier-Barbut, T. Pfau, R. Bombín, J. Sánchez-Baena, J. Boronat, and F. Mazzanti, *Phys. Rev. Res.* **1**, 033088 (2019).
- [55] P. Blakie, A. Bradley, M. Davis, R. Ballagh, and C. Gardiner, *Adv. Phys.* **57**, 363 (2008).